A large-scale radial pattern of seismogenic slumping towards the Dead Sea Basin

G. Ian Alsop and Shmuel Marco

Journal of the Geological Society 2012; v. 169; p. 99-110
doi: 10.1144/0016-76492011-032

Journal of the Geological Society, London, Vol. **169**, 2012, pp. 99–110. doi: 10.1144/0016-76492011-032.

A large-scale radial pattern of seismogenic slumping towards the Dead Sea Basin

G. IAN ALSOP[1]* & SHMUEL MARCO[2]

[1]*Department of Geology and Petroleum Geology, School of Geosciences, University of Aberdeen, Aberdeen AB 3UF, UK*

[2]*Department of Geophysics and Planetary Sciences, Tel Aviv University, Tel Aviv 69978, Israel*

**Corresponding author (e-mail: ian.alsop@abdn.ac.uk)*

Abstract: Although it has been tacitly assumed since the seminal work of Jones in the 1930s that slump folds bear a systematic and meaningful relationship to the slope upon which they were presumably created, there has in reality been very little attempt to objectively verify this association via the collection of regional slump data in a relatively controlled setting. The potential to walk around the intact Dead Sea Basin at *c*. 425 m below mean sea level provides a perhaps unparalleled opportunity to undertake such verification via the direct examination of slump fold relationships. The collection of slump data in this well-constrained environment, where the seismogenic trigger for slumping is established via earthquake records, and the palaeogeographical controls are also recognizable and clearly link to the present bathymetry and landscape, thereby permits an evaluation of the use of slump folds as indicators of palaeoslope. The Late Pleistocene Lisan Formation cropping out to the west of the Dead Sea contains superb examples of slump folds that systematically face (>95%) and verge (>90%) towards the east. This study employs and evaluates five statistical techniques, including a new mean axial-planar dip (MAD) method, to analyse relationships between the orientation of slump folds and palaeoslopes. We recognize for the first time that the direction of slumping inferred from slump folds and thrusts varies systematically along the entire *c*. 100 km length of the western Dead Sea Basin. SE-directed slumping is preserved in the north, easterly directed slumping in the central portion and NE-directed slumping at the southern end of the Dead Sea. They are interpreted to form part of a large-scale and newly recognized radial slump system directed towards the depocentre of the precursor to the Dead Sea, and to be triggered by earthquakes associated with seismicity along the Dead Sea Fault.

The use of slump folds and associated soft-sediment structures to determine the orientation of palaeoslopes (i.e. the direction of dip of the slope) has been widely employed in a number of settings since the pioneering work of Jones (1939). However, the debate on both the usefulness and robustness of a variety of techniques used to estimate palaeoslopes continues (e.g. Lewis 1971; Corbett 1973; Woodcock 1976*a*,*b*, 1979; Potter & Pettijohn 1977; Rupke 1978; Farrell 1984; Maltman 1984, 1994*a*,*b*; Collinson 1994; Bradley & Hanson 1998; Debacker *et al.* 2001, 2009; Strachan & Alsop 2006; Strachan 2008; Alsop & Marco 2011). In addition, improved offshore seismic lines have led to the recognition that relatively recent sediments are also deformed on a large scale via gravity-driven processes creating mass-transfer complexes (MTCs) in slope settings (e.g. see Gardner *et al.* 1999; Lee *et al.* 2007; Bull *et al.* 2009; Jackson 2011). One of the central problems in recognizing and interpreting slump folds and associated palaeoslopes in ancient settings is that subsequent tectonics has frequently complicated and masked the original structural geometries associated with slumping (e.g. Waldron & Gagnon 2011), and the palaeogeographical setting also becomes more difficult to ascertain in older rocks. To overcome these problems we examine slump folds and structures developed in laminated marls of the Lisan Fm, which were deposited in the Late Pleistocene (70–15 ka) precursor to the Dead Sea (e.g. Marco *et al.* 1996; Fig. 1).

The Dead Sea Basin forms a sediment 'sink' currently reaching −750 m below mean sea level, with depths of −425 m at present exposed above water level and therefore accessible for fieldwork. As such, it is the lowest point on Earth at which direct field observations and analysis of structures developed within a basin may be made. This has a number of distinct advantages including the fact that the palaeogeographical setting of the Late Pleistocene Lisan Fm is exceptionally well-constrained around the present Dead Sea Basin (Fig. 1). As such, this may be used as an ideal case study and direct 'controlled' test not only of the use of slump folds as indicators of palaeoslope, but also of the relative complexity and variability that may develop around a pronounced, but relatively simple basin on the scale of *c*. 100 km.

Our study therefore aims to explore a number of factors and fundamental questions pertaining to slumped sediments, including the factors that control the spatial distribution and the transport directions of regional (basin-scale) slump patterns. We thereby evaluate a range of established and new techniques designed to determine the orientation of palaeoslopes from slump fold geometries and orientations. We first present a general overview of fold and fault patterns developed in slump systems, together with a summary of statistical methods used to determine palaeoslope directions from slump folds.

Overview of fold and fault patterns developed in slump sheets

Soft-sediment slump sheets may be considered as deformation cells translating downslope and are typically modelled as displaying extension at the head of the slump balanced by contraction at the lower toe (e.g. Hansen 1971; Lewis 1971; Farrell 1984; Farrell & Eaton 1987; Elliot & Williams 1988; Martinsen 1989, 1994; Martinsen & Bakken 1990; Smith 2000; Strachan 2002; Gilbert *et al.* 2005; Strachan & Alsop 2006; Alsop & Marco 2011). Contractional folds and thrusts developed at the toe of the slump have attracted the most attention in the literature, perhaps because they typically form the most obvious structures, and are also the focus of the present case study. The reader is referred to Alsop & Marco (2011) for a review and details of extensional faulting associated with slumps.

Slump folds may form above flat-lying detachments, where they can be viewed as a variety of flow perturbation folding, broadly

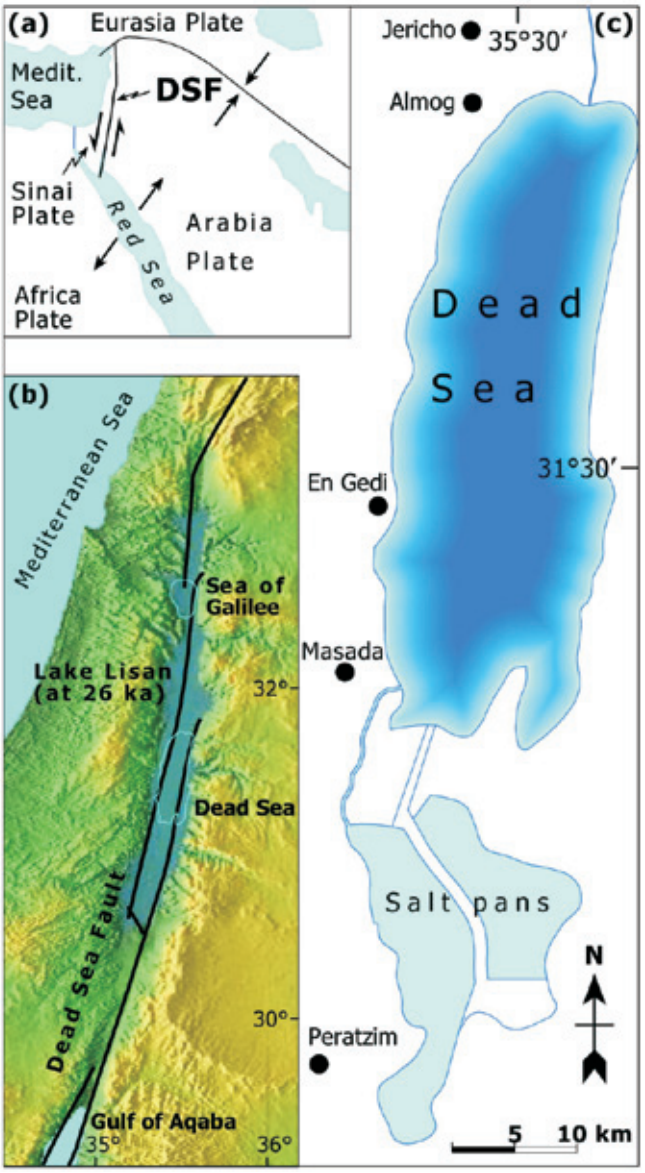

Fig. 1. (**a**) Tectonic plates in the Middle East. General tectonic map showing the location of the present Dead Sea Fault (DSF). The Dead Sea Fault transfers the opening motion in the Red Sea to the Taurus–Zagros collision zone. (**b**) Generalized map showing the maximum extent of Lake Lisan along the Dead Sea Fault at 26 ka. (**c**) Map of the Dead Sea showing the positions of localities referred to in the text and Table 2.

defined as where displacement on an underlying detachment governs the geometry and orientation of the overlying folds (e.g. Coward & Potts 1983; Ridley 1986; Holdsworth 1990; Alsop & Holdsworth 2002, 2004*a*, 2007). Detachments in which displacement is typically uniform along the strike of the slope will create layer-parallel shearing (LPS), which generates folds at high angles to, and verging towards, the downslope flow direction (e.g. Alsop & Holdsworth 2007; Fig. 2). Conversely, detachments marked by pronounced gradients in displacement along the strike of the slope will create layer-normal shearing (LNS), which initiates folding oblique or subparallel to the flow direction (e.g. Strachan & Alsop 2006; Alsop & Holdsworth 2007; Debacker *et al.* 2009; Alsop & Marco 2011).

As a result of variations in the LPS and LNS components of flow in slump sheets, it may be found that slump folds display broadly arcuate traces about the flow direction. In addition, slump folds may subsequently undergo hinge and axial-planar rotations during continued downslope movement to create curvilinear sheath fold geometries (e.g. Alsop & Holdsworth 2004*b*, 2006; Alsop & Carreras 2007; Alsop *et al.* 2007; Fig. 2). Further complications may include local backthrusts and folds verging up the palaeoslope, together with attenuation of fold limbs (Fig. 2; for further details see Alsop & Marco 2011). We now summarize and evaluate the main statistical methods of determining palaeoslopes from slump fold geometries before applying these to the Dead Sea Basin.

Statistical methods to determine palaeoslope directions from slump folds

A variety of techniques have been developed to deduce the direction of a palaeoslope from the orientation of slump folds. These techniques have recently been reviewed by Strachan & Alsop (2006), Alsop & Holdsworth (2007) and Debacker *et al.* (2009) and we therefore only provide brief descriptions below and summaries in Table 1.

Fold facing directions

Fold facing is defined as the direction, normal to the fold hinge and along the axial plane, in which younger rocks are encountered (see Holdsworth 1988). As with fold vergence it is given a directional notation (west, east, etc.), but it is also noted if the facing direction has an upward or downward component (Fig. 3). The facing direction represents a line that plots as a point on a stereonet (Fig. 3). Downward-facing lines intersect the standard lower hemisphere of a stereonet and are directly plotted as points (see Holdsworth 1988), whereas upward-facing lines intersect the upper hemisphere of the stereonet and are simply projected vertically down to plot on the lower hemisphere as chordal points (Fig. 3; see Alsop & Marco 2011). Woodcock (1976*a*) recognized that slump folds will typically face upwards and verge towards the downslope flow direction. Facing therefore represents a valuable tool in deciphering slump folds, as downward-facing folds are atypical and may represent critical areas of refolding (Woodcock 1976*a*).

The mean axis method (MAM)

It has been recognized since the work of Jones (1939) that fold hinges may form at right angles to the downslope direction and form statistical groupings normal to the flow or slump direction. This mean axis method (MAM) has been recently reviewed by Strachan & Alsop (2006), Alsop & Holdsworth (2007) and Debacker *et al.* (2009). Although this simple fold–slope relationship may be complicated by differential LNS, resulting in a range of both transport subparallel and transport-normal fold hinges, it is apparent that such complications may be readily identified via the detailed examination of geometric relationships associated with fold vergence and asymmetry (see Alsop & Holdsworth 2002, 2004*a*,*b*, 2007; Table 1). In areas of marked differential movement associated with LNS, fold hinges may initiate subparallel to transport and display asymmetries in both directions (S and Z folds) to define bimodal vergence patterns (Table 1) (for a full review see Alsop & Holdsworth 2007). Conversely, in areas of marked LPS but only limited LNS, fold hinges initiate at right angles to transport and display a consistent sense of asymmetry to define unimodal vergence patterns (Table 1). Clearly, the MAM is most suited to areas where layer-parallel shear dominates and little subsequent fold rotation has occurred.

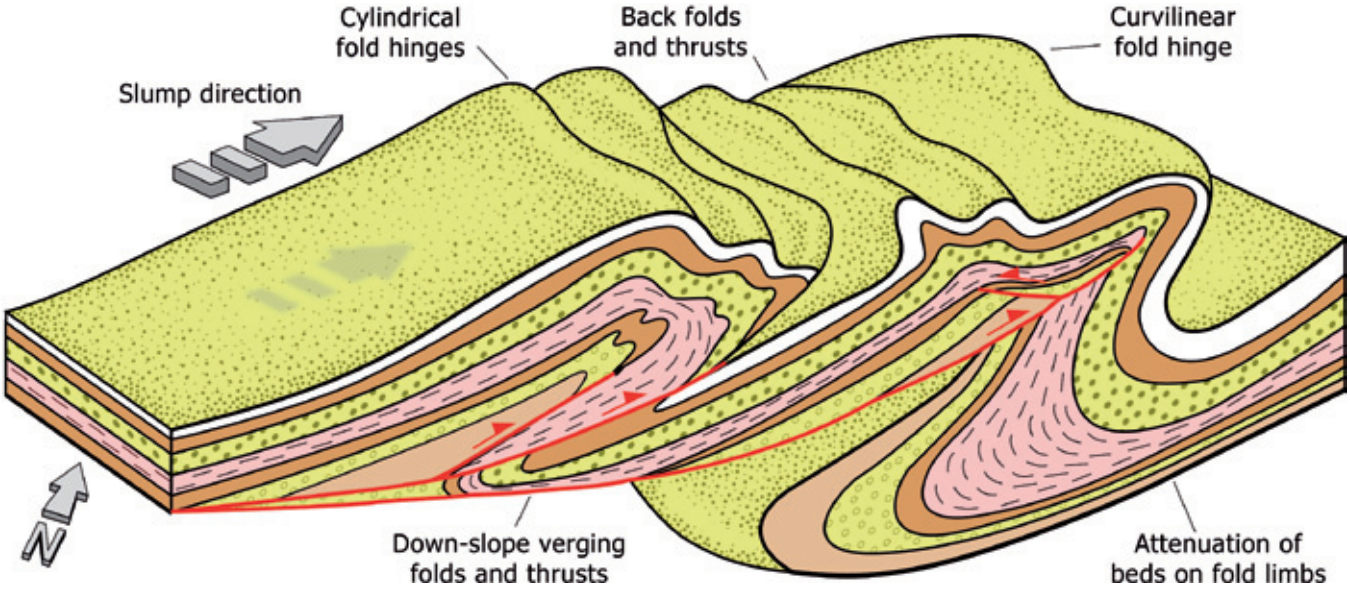

Fig. 2. Schematic illustration of typical fold and thrust geometries generated during slumping. Folds may display cylindrical to gently curvilinear hinges and are predominantly downslope verging, although back-folds and thrusts verging upslope may also develop. Interplay between folds and thrusts may result in locally complex cut-off geometries associated with back-collapse down the oversteepened limbs (for further details see Alsop & Marco 2011).

Table 1. *Assumptions and associated problems of five methods of determining palaeoslope from fold data*

	Mean axis method (MAM)	Mean axial plane strike method (MAPS)	Mean axial-planar dip method (MAD)	Separation arc method (SAM)	Axial-planar intersection method for LPS (AIM)	Axial-planar intersection method for LNS (AIM)
Assumption 1	Fold hinges will verge and face downslope	Fold hinges will verge and face downslope	Fold hinges will verge and face downslope	Fold hinges will verge and face in a downslope arc	Fold axial planes will fan and dip upslope	Fold axial planes will fan and dip about the downslope direction
Assumption 2	Flow direction is normal to the mean fold axis trend	Flow direction is normal to the mean axial plane strike	Flow direction is normal to mean fold axis trend associated with steep axial plane dips	Flow direction bisects acute angle between folds with opposing vergence	Flow direction is normal to the fanning axial planes	Flow direction is parallel to the fanning axial planes
Problem 1	Does not allow for downslope (i.e. flow-parallel) fold axes	Does not allow for downslope (i.e. flow-parallel) fold axes and axial planes	Does not allow for downslope (i.e. flow-parallel) fold axes and axial planes	Does not allow for overlapping fold distributions	Requires careful 3D evaluation of folding	Requires careful 3D evaluation of folding
Problem 2	Skewed distributions not differentiated by means	Skewed distributions not differentiated by means	Skewed distributions not differentiated by means	Based on extreme end-member fold orientations	Unimodal axial-planar dip distribution requires even sampling	Bimodal axial-planar dip distribution requires even sampling

It should be noted that the axial-planar intersection method (AIM) is separated into settings involving layer-parallel shear (LPS) and layer-normal shear (LNS).

The mean axial plane strike method (MAPS)

This technique is a development of the mean axis method noted above and simply employs the mean strike of axial planes (rather than the trend of associated fold axes) to determine the transport direction (Table 1). The relationship of axial-planar strike with the transport direction in both LPS- and LNS-dominated extensional and contractional systems has been discussed at length by Alsop & Holdsworth (2007). In systems governed by LNS, axial planes will strike normal to the trend of the palaeoslope and parallel to the downslope direction (Table 1). Within systems dominated by LPS, the strike of axial planes will form a statistical grouping parallel to the trend of the palaeoslope and normal to the downslope direction (Table 1). The strike of slope-parallel and slope-normal axial planes will vary little during progressive deformation in LPS and LNS settings respectively, as rotation of axial planes into the shear plane will simply affect the dip of these surfaces (see the section below).

The mean axial-planar dip method (MAD)

This new method utilizes the trend of fold hinges together with the angle of dip of associated axial planes and is based on methods used by Strachan (2002) (Table 1). Statistical fanning of axial planes

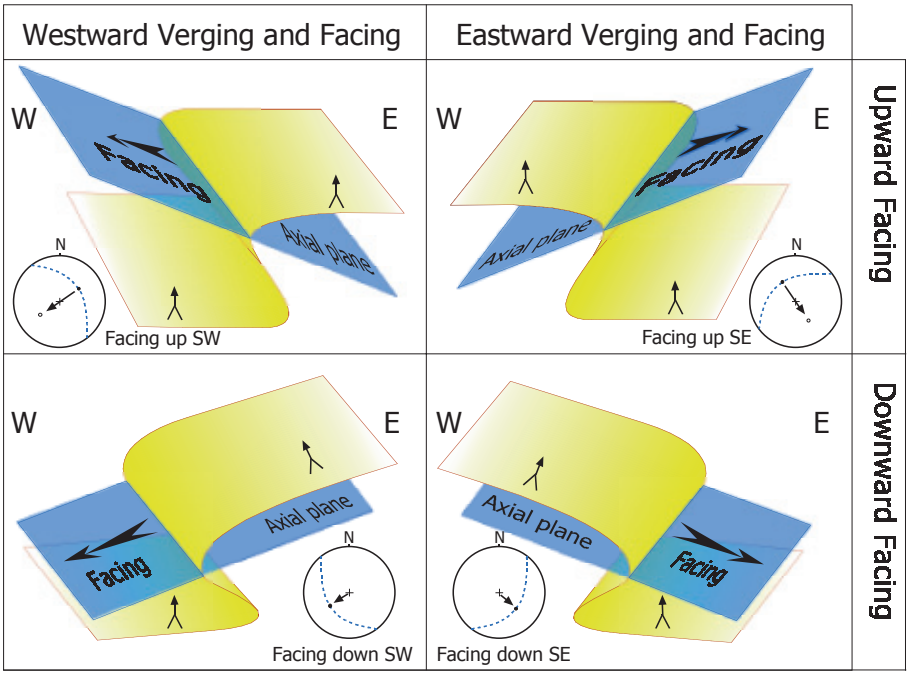

Fig. 3. Schematic diagrams summarizing the various relationships between fold vergence, way-up of beds (shown by the younging arrows), axial planes and either upward- or downward-facing scenarios. Related stereoplots show the axial plane as a great circle, the direction of facing as an arrow and the facing line as a dot. Where folds are upward-facing, the facing line would intercept the upper hemisphere, and is therefore projected vertically down and plotted as a chordal point (open circle) on the lower hemisphere of the stereoplot (for details, see Alsop & Marco 2011).

about the strike of the palaeoslope, with the majority of planes dipping in an upslope direction, has been long recognized (e.g. Woodcock 1979). This fanning of axial planes is typically considered to represent the effects of shearing and rotation of earlier upright folds during progressive deformation, and is consistent with overall layer-parallel shear (Alsop & Holdsworth 2004*a*; Strachan & Alsop 2006; Alsop & Carreras 2007; Lesemann *et al.* 2010). More steeply dipping axial planes are considered to have undergone less significant rotation during subhorizontal shearing, and the fold hinges associated with these steep axial planes therefore more closely preserve the original fold trend. Restricting the use of fold hinges to those associated with steeper axial planes (typically >45° relative to non-deformed beds) statistically removes fold hinges that may have undergone more significant rotation during progressive deformation. Thus, the most steeply dipping axial planes are least rotated, and the associated fold hinges should form normal to the downslope transport direction in LPS-dominated settings (Table 1). In LNS-dominated settings associated with large amounts of differential shear, the steeper axial planes are typically considered to develop subparallel to the downslope transport direction and be associated with tighter interlimb angles (e.g. Alsop & Holdsworth 2007; Debacker *et al.* 2009). Therefore a clear understanding of whether a system is dominated by LPS or LNS is essential.

The separation arc method (SAM)

The separation arc method (SAM) of Hansen (1971) is based on the observation that folds may display highly variable hinge orientations about the palaeoslope direction. This technique assumes that the flow direction will symmetrically bisect the acute angle between groups of folds that display opposing asymmetry or vergence (Table 1). Thus, folds that are developed clockwise of the downslope flow direction will typically be associated with differential sinistral shear, whereas anticlockwise folds are marked by differential dextral shear (for a full review see Alsop & Holdsworth 2007). The main weakness of the method is that it relies solely on extreme end-member fold orientations to constrain the arc of separation, and is thus heavily dependent on overall sampling issues (see Woodcock 1979). The method becomes non-applicable when (1) folds with opposing vergence define statistically overlapping distributions, thereby rendering the 'separation arc' with which to constrain flow inoperable, or (2) only one sense of fold vergence is observed owing to either real or apparent gross fold asymmetry, thereby once again negating any separation arc with which to constrain the flow direction (Table 1).

The axial-planar intersection method (AIM)

The axial-planar intersection method (AIM) was originally devised by Alsop & Holdsworth (2002, 2004*a*,*b*) for flow perturbation folds and subsequently applied to slumps by Strachan & Alsop (2006) and Debacker *et al.* (2009). The AIM utilizes the statistical orientation of fold axial planes to determine both the trend and direction of flow associated with slumping. Within LNS-dominated slump systems, axial planes will trend subparallel to the flow direction, and define a statistical fan with the mean intersection of axial planes parallel to the downslope direction (Table 1). Within LPS-dominated slump systems, axial planes will trend at high angles to the transport direction. They will define a statistical fan with the majority of axial planes variably dipping upslope (Woodcock 1979), and relatively few dipping in the downslope direction (as a result of subsequent warping and rotations). The general trend of variably dipping axial planes parallel to the strike of the palaeoslope will result in the calculated intersections between fanning axial planes also forming parallel to the strike of the palaeoslope (Woodcock 1979; Table 1).

Regional setting of the Dead Sea Basin case study

The Dead Sea Basin represents an exceptional area to analyse slump folds as it is located on the Dead Sea transform, which is marked by two parallel fault strands that generate numerous earthquakes with which to trigger slumping (e.g. Marco *et al.* 1996, 2003; Ken-Tor *et al.* 2001; Migowski *et al.* 2004; Begin *et al.* 2005; Kagan *et al.* 2011; Fig. 1a). This transform is thought to have been active since the Miocene (e.g. Bartov *et al.* 1980; Garfunkel 1981). In addition, the pronounced bathymetry of the present Dead Sea (reaching −750 m

Table 2. *Mean fold axis and axial-planar orientations with calculated slump transport directions for the Lisan Fm*

Name, number of data (*n*) and GPS location	Mean axis method (MAM)	Mean axial plane strike method (MAPS)	Mean axial-planar dip method (MAD)	Axial-planar intersection method (AIM)	Separation arc method (SAM)	Mean facing direction (FD)	Average of 5 methods (MAM + MAP + MAD + AIM + SAM)	Bisector of 5 methods (MAM + MAP + MAD + AIM + SAM)
Jericho (*n* = 9) (31°4758.2N, 35°3031.2E)	TD 127° (09/037); 100% FA verge E	TD 140° (050/46^{W}); 0% AP dip E	TD 133°; mean FA trend on steeper AP (dips >45°) = 043°	TD 133° (07/043)	n.a. (single fold vergence datum)	FD 114° (43/114); 100% face up SE	TD 134° (SE-directed slumping)	TD 134 ± 7°; range 127–140° (SE-directed slumping)
Almog (*n* = 46) (31°4751.8N, 35°2715.3E)	TD 090° (00/000); 100% FA verge E	TD 085° (175/23^{W}); 9% AP dip E	TD. 096°; mean FA trend on steeper AP (dips >45°) = 006°	TD 091° (03/181)	TD 091° (082° arc from 050° to 132°)	FD 91° (30/091); 94% face up SE	TD 091° (E-directed slumping)	TD 091 ± 6°; range 085–096° (E-directed slumping)
En Gedi (*n* = 12) (31°3543.7N, 35°2414.0E)	TD 075° (13/165); 83% FA verge E	TD 069° (159/09^{W}); 0% AP dip E	TD 080°; mean FA trend on steeper AP (dips >20°) = 170°	TD 064° (10/244)	TD 043° (055° arc from 015° to 070°)	FD 68° (12/068); 91% face up ENE	TD 066° (ENE-directed slumping)	TD 062 ± 19°; range 043–080° (ENE-directed slumping)
Masada (*n* = 55) (31°1847.0N, 35°2228.3E)	TD 074° (01/164); 100% FA verge E	TD 073° (163/10^{W}); 0% AP dip E	TD 083°; mean FA trend on steeper AP (dips >20°) = 173°	TD 075° (0/165)	TD 082° (085° arc from 040° to 125°)	FD 76° (10/076); 100% face up ENE	TD 077° (ENE-directed slumping)	TD 078 ± 5°; range 073–083° (ENE-directed slumping)
Peratzim (*n* = 235) (31°0449.6N, 35°2104.2E)	TD 045° (01/315); 89% FA verge E	TD 036° (126/09^{W}); 17% AP dip E	TD 034°; mean FA trend on steeper AP (dips >45°) = 124°	TD 046° (1/136)	n.a. (overlapping fold vergence data)	FD 42° (14/042); 94% face up NE	TD 040° (NE-directed slumping)	TD 040 ± 6°; range 034–046° (NE-directed slumping)

Analysis is based on mean axis method (MAM), mean axial plane strike method (MAPS), mean axial-planar dip method (MAD), axial-planar intersection method (AIM) and separation arc method (SAM) for each station (from north to south) along the western shore of the Dead Sea. The mean fold facing direction (FD) is also calculated for each station. Calculated transport directions (TD) from bisectors and averages of the five methods are also shown. n.a., not applicable. AP, axial plane; FA, fold axis.

below sea level) mirrors that of the Late Pleistocene Lake Lisan (which acts as the precursor to the Dead Sea) and is the focus of the current study (Fig. 1b). As both the seismic triggering mechanism for slumping and palaeogeographical control on slump directions are equally well constrained, this provides an ideal opportunity to evaluate slump folds as indicators of palaeoslope.

The Lisan Fm comprises a sequence of finely laminated annual varve-like repetitions of aragonite and clastic-rich pairings considered to represent dry summers and winter flood events respectively (Begin *et al.* 1974). The Lisan Fm was deposited between 70 and 15 ka (Haase-Schramm *et al.* 2004) and preserves depositional dips of less than 1° indicating an absence of subsequent tilting and tectonism. The end of the last ice age brought about a sharp drop of water level at *c.* 15 ka, forming the hypersaline Dead Sea in the lowest place, which had also acted as the depocentre of Lake Lisan (Fig. 1b and c).

Within the Lisan Fm, folding and thrusting in distinct layers that are capped by overlying undeformed horizontal beds is relatively common (see Alsop & Marco 2011). These intraformational deformed horizons are subsequently cut by sedimentary injections, proving the syndepositional nature of the 'soft-sediment' deformation. The folded horizons are frequently capped by breccia layers, which also abut syndepositional faults indicating that the breccia layers are associated with deformation of the sea floor and are seismites (Marco & Agnon 1995; Agnon *et al.* 2006). The breccia layers are considered to be the final stage in a progressive sequence of deformation that initiated with laminar folds, which evolved into asymmetric billows and finally turbulent chaotic breccias (Heifetz *et al*. 2005; Wetzler *et al.* 2010). We now present new slump fold data from along the entire western shore of the Dead Sea with which to directly test if the geometry and orientation of the folds accurately reflects downslope slumping of sediments towards the Dead Sea Basin.

Detailed observations of slump fold geometries and orientations within the Lisan Fm

We have documented and recorded >350 representative folds from all the available outcrops of the Lisan Fm on the western shore of the Dead Sea from Jericho in the north to Peratzim in the south (Fig. 1c). For these measurements we utilized natural outcrops on numerous canyon walls that are incised into the Lisan Fm. To determine the true geometry of the fold hinges, we carefully excavated them in three dimensions in the little consolidated sediments, and then labelled and photographed each of them. In all photographs, west is on the left and east is on the right (unless stated otherwise), and the hammer (30 cm long), paper ruler (20 cm long) and coin (15 mm diameter) act as scales. The global positioning system (GPS) coordinates for each of the stations are provided in Table 2.

A description of slump folding from each site within the Lisan Fm down the western shore of the Dead Sea is provided below, including the orientation, geometry, scale, tightness of folds and typical fold vergence directions (Figs 1c and 4). We apply the various techniques of palaeoslope analysis described above, before summarizing the regional slump patterns along the *c*. 100 km transect of the western Dead Sea Basin. Results from the five techniques are analysed via mean slump directions, and also by calculating the spread of slump transport directions and taking the bisector of this range with appropriate errors noted (see Debacker *et al.* 2009).

Jericho

Slump folds at Jericho by the northern Dead Sea are <10 cm amplitude, 15–20 cm wavelength, upright to recumbent folds,

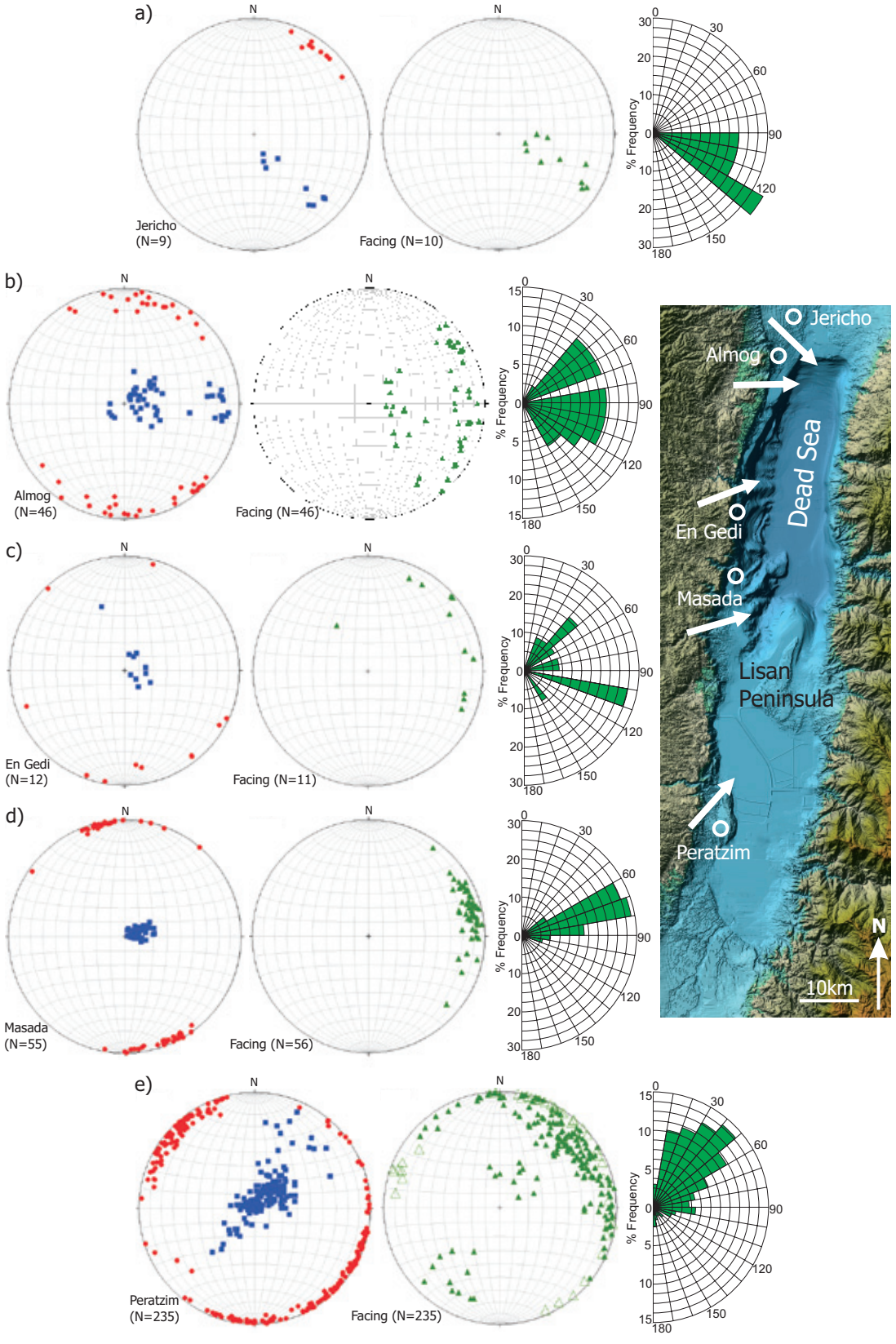

Fig. 4. Equal area stereoplots of fold hinges (red circles), axial surfaces (blue squares) and facing directions (green triangles). Downward-facing directions are shown by open green triangles. Upward-facing directions are plotted as filled green triangles, which are projected vertically down (as chordal points) from their upper hemisphere intersection onto the lower hemisphere stereonet. Facing trends are also shown on the associated rose diagrams. Data were collected from the Lisan Fm on the western shores of the Dead Sea at (**a**) Jericho, (**b**) Almog, (**c**) En Gedi, (**d**) Masada and (**e**) Peratzim. Locations of these sites are shown on the associated map, together with interpreted mean slump directions (white arrows).

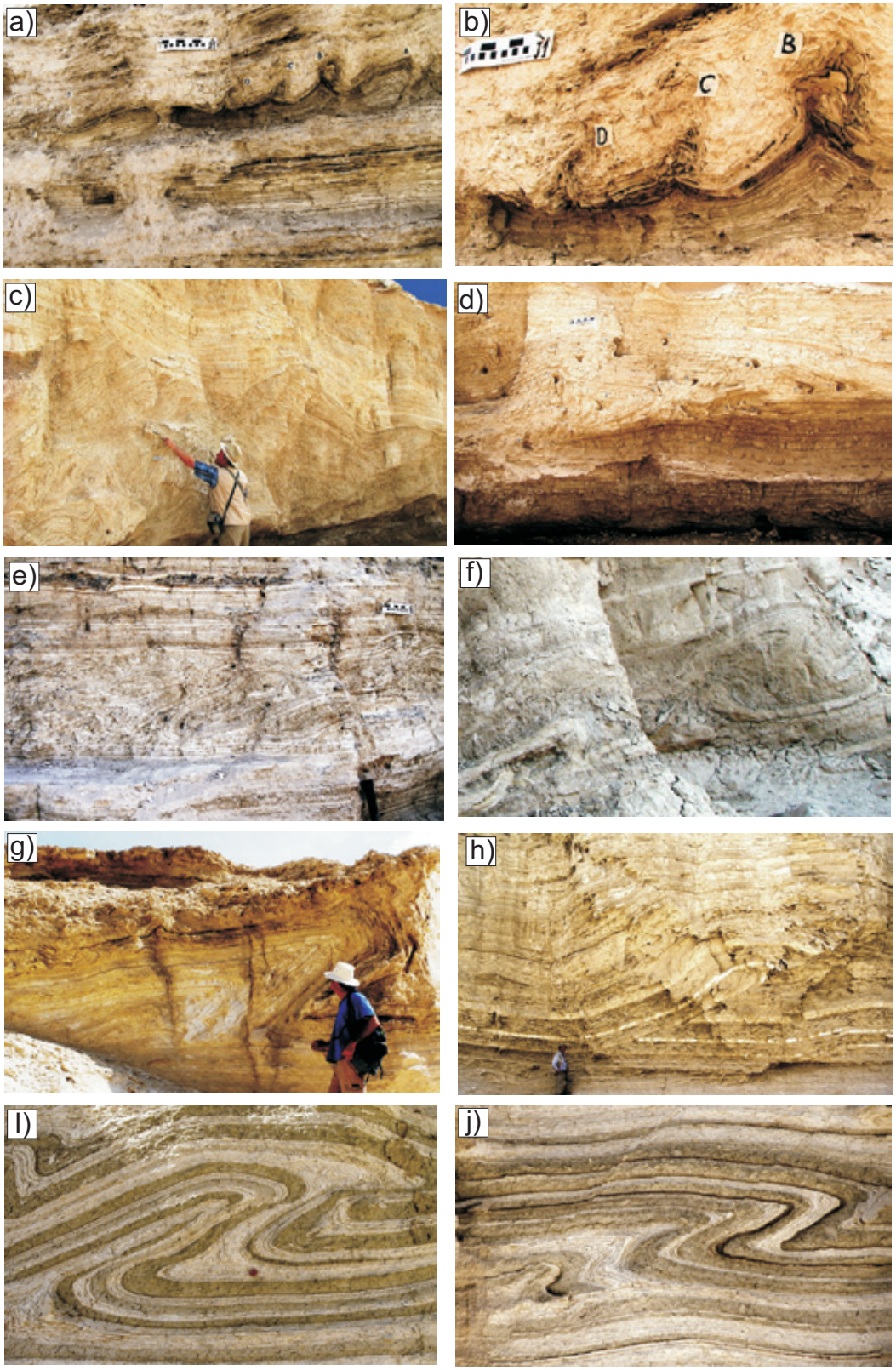

Fig. 5. Photographs of slump folds and thrusts developed in the Lisan Fm down the western shore of the Dead Sea. All photographs have been orientated such that the eastern quadrant is towards the right-hand side of the photograph. Details of GPS coordinates for each site are given in Table 2. (**a**, **b**) Upright slump folds developed at Jericho showing angular hinges. (**c**, **d**) Slumped sequence containing folds and thrusts, which are truncated and overlain by undeformed horizontal beds at Almog. The overlying sequence locally thickens and infills the irregular erosive surface, and displays some sedimentary draping that may have been enhanced by subsequent compaction. (**e**, **f**) East-verging slump folds at En Gedi. (**g**) East-verging slump fold at Masada. (**h**) East-directed thrust within a 5 m high sequence of Lisan Fm at Masada. Displacement along the thrust dies out upwards into folds. (**i**, **j**) NE-verging recumbent slump folds developed at Peratzim.

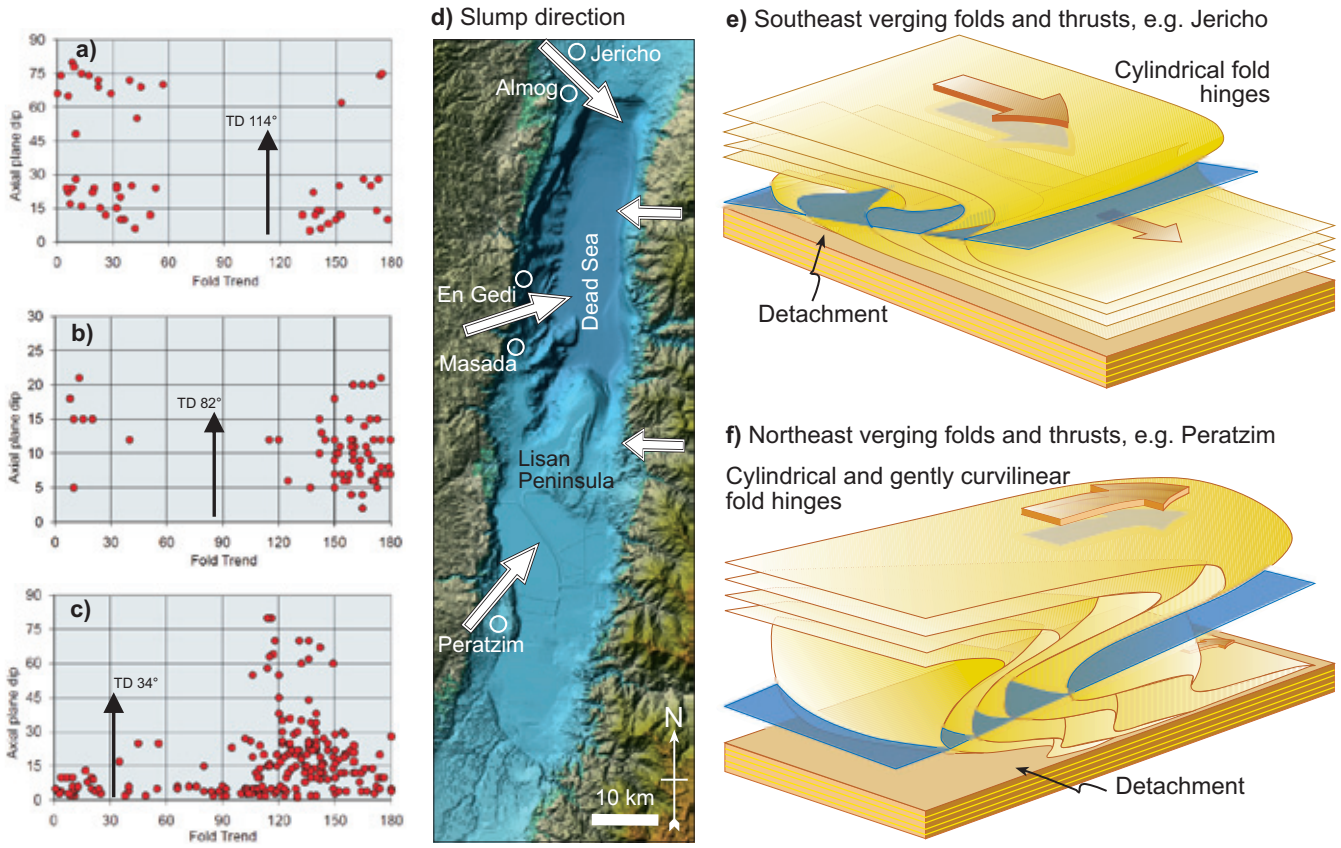

Fig. 6. Plots showing the trend of fold hinges relative to axial-planar dip from (**a**) Jericho and Almog by the northern Dead Sea. (**b**) En Gedi and Masada by the central Dead Sea, (**c**) Peratzim at the southern end of the Dead Sea (refer to Fig. 1c for location). The calculated transport direction (TD) is shown by the black arrow in each case. (**d**) Map of the Dead Sea showing mean slump directions (white arrows) in the northern, central and southern sections (refer to **a**–**c** for data). Slump directions on the eastern side of the Dead Sea are directly towards the west and based on the observations of El-Isa & Mustafa (1986). (**e**, **f**) Schematic 3D illustrations illustrating fold geometries from the Lisan Fm. (**e**) In the northern portion of the Dead Sea (e.g. Jericho and Almog) folds and thrusts are typically SE-verging with axial planes (shown in blue) gently to moderately inclined towards the west and NW. (**f**) In the southern portion of the Dead Sea (e.g. Peratzim) folds and thrusts verge towards the NE, with some hinges within mud-rich units displaying gentle to moderate curvilinear geometries.

which typically tighten as they become recumbent (Fig. 5a). Upright folds are generally slightly more angular with some evidence of brittle deformation in the hinge associated with limb failure (Fig. 5b). Fold hinges are NE–SW-trending with axial planes displaying a range of shallow to steep NW-dipping orientations, although the NE–SW strike remains relatively constant (Figs 4a and 6a, Table 2). Fold facing directions are consistently up towards the SE, subparallel to the calculated palaeoslope direction towards 134° (Table 2). The range of transport directions calculated from the five techniques varies between 127° and 140° with an overall mean bisector towards 134 ± 7° (Table 2).

Almog

Slump folds at Almog by the northern Dead Sea are <1 m amplitude, <1 m wavelength, upright to recumbent folds, which tighten as they become overturned (Fig. 5c and d). Exposures at Almog also preserve the highly irregular top surface of a slump, which is draped by overlying undeformed sediments that display pronounced thickening and thinning over the slumped horizon (Fig. 5c). Fold hinges are typically north–south-trending, although they display an arc of orientations (Figs 4b and 6a). Axial planes show a range of shallow to steep west-dipping orientations, although the north–south strike remains relatively constant (Figs 4b and 6a, Table 2). Fold facing is marked by a range of NE to SE directions, although the mean is parallel to the calculated palaeoslope direction towards 091° (Table 2). The range of transport directions calculated from the five techniques varies between 085° and 096° with an overall mean bisector towards 091 ± 6° (Table 2).

En Gedi

Slump folds at En Gedi by the central Dead Sea are <0.5 m amplitude, <0.5 m wavelength, recumbent folds with rounded hinges that display distinct asymmetry with thinning of fold limbs relative to the hinge (Fig. 5e and f). Fold hinge orientations are widely dispersed, although they are generally SE–NW- to SW–NE-trending and typically ENE-verging (Figs 4c and 6b, Table 2). Axial planes are SSE-striking and dip gently towards the west, with associated fold facing up and towards the ENE (068°), subparallel to the calculated palaeoslope direction (Figs 4c and 6b, Table 2). The range of transport directions calculated from the five techniques varies between 043° and 080° with an overall mean bisector towards 062 ± 19° (Table 2). The larger spread (37°) in calculated slope directions is considered to reflect the relatively small dataset at this site.

Masada

Slump folds at Masada by the central Dead Sea are up to 2 m amplitude and 2 m wavelength, although more typically <0.25 m (Fig. 5g). They display a range of upright to sub-recumbent attitudes marked by well-defined asymmetry and vergence (Fig. 5g). Larger-scale thrusts associated with easterly directed thrusting display up to *c*. 5 m displacement with back-rotation of the thrust slice being accommodated by folding of up to 5 m of overlying sediment (Fig. 5h). These observations suggest that, in some cases, significant thicknesses and volumes of sediment may be affected by single slump events. Fold hinges are concentrated around a NNW–SSE trend and verge consistently towards the east (Fig. 4d, Table 2). Axial planes are SSE-striking and dip gently towards the west, with associated fold facing up and towards the ENE (076°), subparallel to the calculated palaeoslope direction (Figs 4d and 6b, Table 2). The range of transport directions calculated from the five techniques varies between 073° and 083° with an overall mean bisector towards 078 ± 5° (Table 2).

Peratzim

Slump folds at Peratzim by the southern Dead Sea are typically <1 m wavelength and form in packages less than 1 m thick, although some thrust sequences can be 2 m thick. Folds are upright to more typically recumbent with rounded hinges (Fig. 5i and j). Fold hinges are statistically distributed around a broad arc, although fewer hinges are recorded in a NE–SW orientation (Figs 4e and 6c, Table 2). Axial planes are SE–NW-striking and typically dip gently towards the SW, although steeply SW-dipping axial planes are also recorded (Figs 4e and 6c, Table 2). This range of fold hinge and axial-planar orientations is considered a consequence of their rotation towards the downslope transport direction during progressive deformation associated with downslope slumping (see Strachan & Alsop 2006). A minority of axial planes are gently NE-dipping and may be associated with marginally (typically <10°) downward-facing folds, possibly related to gentle warping and refolding during slumping. The vast majority (>94%) of folds face up towards the NE (Table 2). Fold axes associated with axial planes that dip moderately to steeply SW (>45°) are all SE–NW-trending (mean 124°), suggesting that the palaeoslope direction would be towards 034° (using mean axial-planar dip) (Fig. 6c and d, Table 2). The general facing direction, although displaying an arc of orientations, is broadly unimodal towards 042° and subparallel to the assumed palaeoslope direction (Figs 4e and 6c, Table 2). The range of transport directions calculated from the five techniques varies between 034° and 046° with an overall mean bisector towards 040 ± 6° (Table 2).

Regional patterns of radial slumping towards the Dead Sea Basin

On a regional scale, our results show that the Late Pleistocene Lisan Fm on the western side of the Dead Sea displays SE-directed slumping in the north (Fig. 6d and e), easterly directed slumping in the central portion and NE-directed slumping at the southern end of the Dead Sea (Fig. 6d and f). The direction of slumping inferred from the fold and thrust geometries therefore systematically varies along the entire length of the western Dead Sea (Fig. 6d).

Seilacher (1984) and El-Isa & Mustafa (1986) discussed soft-sediment deformation structures from within the Lisan Fm exposed along the eastern side of the Dead Sea. They described folds with amplitudes up to 15 cm and wavelengths of 17 cm, which are fairly constant within single localities. On the eastern side of the Dead Sea, El-Isa & Mustafa (1986) described the inclination of detachments as 'mostly, if not always, westwards' and minor folds as displaying 'systematic westward inclination' relating to west-directed vergence (Fig. 6d). Such folded horizons are capped by undeformed beds both above and below, and were attributed by El-Isa & Mustafa (1986) to earthquakes triggering slumps on very gentle westerly dipping slopes. Collectively, the directions of slumping ascertained from folds and thrusts within the Lisan Fm exposed around the western and eastern shores of the Dead Sea define a pronounced radial pattern of slumping towards its depocentre (Fig. 6d).

Discussion

Regional fold vergence and facing patterns

Lake Lisan was bounded by the same fault system that bounds the Dead Sea, with the studied outcrops of the Lisan Fm typically within 5 km of the Dead Sea Fault (Figs 1 and 6d). The present bathymetry, which is similar to that of Lake Lisan, is shown in Figures 4 and 6d. These maps highlight the position of the studied localities on very gentle slopes, with the main depocentre located further to the east in the northern part of the Dead Sea. This depocentre, which is marked by a sharp bathymetric break, is considered to be fault bounded (e.g. Lazar *et al.* 2006). Bedding dips within the Lisan Fm are <1° and reflect original depositional slopes within Lake Lisan. Slopes of 1° are typically considered sufficient to develop slumping within many subaqueous settings (e.g. Lewis 1971; Almagor & Garfunkel 1979; Canals *et al.* 2004), and seismicity has also been recognized as a trigger for slumping within lake sediments (e.g. Doig 1991; Doughty *et al.* 2010). The direction of palaeoslope inferred from slump folding defines a radial pattern directed towards this depocentre. A coherent regional slump pattern across the Dead Sea indicates a lack of secondary tectonic control on slope directions such as associated with locally tilted fault blocks.

Fold vergence on the western shore of the Dead Sea is systematically (>90%) towards the east. Furthermore, mean fold facing directions display a unimodal distribution (>95% face up towards the east) and are consistently subparallel to the mean transport direction calculated from the five techniques at each site. This marked consistency in both fold vergence and facing directions is to be expected in areas where LPS dominates (Alsop & Holdsworth 2004*b*, 2007). Within LPS systems, the strike of fold axial planes will parallel the trend of the palaeoslope and dips are typically directed upslope (Fig. 6e and f). Axial-planar dips directed to the east (downslope) may be associated with subsidiary west-vergent folds, or subsequent rotations through the horizontal with continued movement and contraction. The small percentage (<10%) of folds verging towards the west up the regional slope reflect secondary structures generated by local slumping off the bathymetric 'highs' generated by the crests of underlying antiforms and thrust culminations (Alsop & Marco 2011). In areas where differential layer-normal shear operates, folds with opposing vergence are typically developed in equal proportions around classic flow perturbations. The strike of fold axial planes in such systems will parallel the transport direction. The extreme asymmetry of fold vergence (>90% verging east) and axial-planar dip directions indicates the dominance of layer-parallel shear in the present case study (Figs 4–6, Table 2).

Wetzler *et al.* (2010) suggested that the Kelvin–Helmholtz instability, where folding is triggered by shear between stably stratified layers, is a plausible mechanism for folding in the Lisan Fm as it requires only a small perturbation in the interface between sheared

layers. This shear instability is considered to grow and evolve through the folding stages up to a turbulent breccia (see Wetzler *et al.* 2010; Alsop & Marco 2011). Wetzler *et al.*'s model does not attempt to explain all of the folds and those workers did not analyse fold vergence or transport directions. Our work clearly now demonstrates that the sense of fold vergence and associated transport direction is dictated by the palaeoslope.

The use of slump folds as indicators of palaeoslope

Relationships between slump folds and palaeoslope orientations may be complicated by a number of factors including the following: (1) variable angles of fold initiation; (2) variable amounts of fold hinge and axial-planar rotation towards the transport direction; (3) variable overprinting relationships between adjacent slumps; (4) variable slope or transport directions that may evolve with time. These complications are very similar to many of those encountered in ductile metamorphic shear zones, where the concepts of progressive shearing coupled with flow perturbations have allowed meaningful deformation analyses to be undertaken (e.g. see review by Alsop *et al.* 2010).

Within this case study, there is little evidence of folds initiating at variable angles to the downslope transport direction. This indicates that deformation is dominated by LPS, perhaps reflecting the layer-cake stratigraphy of the Lisan Fm, which lacks lateral facies changes that would encourage along-strike partitioning of flow (see discussion by Alsop & Marco 2011). Thus, fold hinges and associated axial planes typically initiate at high angles to the downslope direction. In addition, fold hinge and axial-planar rotation towards the transport direction during progressive deformation appears relatively limited, and mostly restricted to intensely deformed horizons at Peratzim where some curvilinear folding is observed (Figs 4e and 6f). We attribute the development of curvilinear folds at Peratzim as reflecting an increased component of mud-rich units that are relatively weak and would encourage more intense folding to form (see Alsop & Marco 2011, p. 453, for full details). Overall, fold hinges and axial planes maintain high angles to the slope direction, although rotation of axial planes about their strike allows fanning geometries to be utilized in slope analysis. There is also little evidence of overprinting relationships between laterally adjacent slumps that may otherwise result in reworking and reorientating of slump folds.

Recent slump analogues from seismic reflection and sea-floor data

Recent submarine examples of slumped zones include the Humboldt Slide, where large bowl-like depressions or 'ampitheatres' are imaged (e.g. Lee *et al.* 2007). In this case, the bathymetric ridges trend directly across the basin and do not parallel the geometry of the bowl. However, these ridges form at wavelengths of hundreds of metres and are several orders of magnitude larger than folds described from the Lisan Fm. In addition, they may relate to sediment wave fields rather than landslides or slumping processes (see Gardner *et al.* 1999, and discussion by Lee *et al.* 2007).

Detailed analysis of seismic reflection data from sub-lacustrine landslides reveals radial patterns of slope failure that converge towards the centre of a *c.* 2.5 km diameter volcanic crater lake (Moernaut & De Batist 2011). Slumped units extend for up to 500 m and display extensional faulting towards the upslope margins and contractional folds and thrusts in the toe of the slumps towards the downslope centre of the basin. This pattern is repeated at different stratigraphic levels with palaeoslope dips of just *c.* 2° to form a coherent radial system. Angles of palaeoslope, coupled with the extent of single slumps and the overall radial pattern within a confined basin setting dominated by lacustrine sediments, allow analogies to be drawn with the Lisan Fm case study. Although details of folding and faulting are limited by seismic resolution, our direct observations of slump folds and their associated regional patterns allow greater controls and confidence to be placed on such seismically imaged systems.

In summary, many of the factors that create complexity within slump systems are absent or minimized within the Dead Sea Basin, thereby allowing original and pristine relationships to be observed and investigated. The clear control exerted by the geometry of the pronounced Dead Sea Basin from the Late Pleistocene, when the Lisan Fm was deposited, to the present day, when bathymetry reaches −750 m, has allowed us to evaluate the viability of slump folds as indicators of slope direction. Importantly, we can directly observe how transport directions vary around a relatively simple and recent system, where the palaeogeographical control is still evident. Our direct field observations also allow greater confidence to be placed in seismically imaged structures defining convergent and radial systems of slumping.

Conclusions

Detailed fieldwork in the Dead Sea Basin has allowed us to objectively test if slump folding accurately reflects palaeoslope orientations over a regional scale. The results of this work clearly indicate that the sediments along the present western shore of the Dead Sea slumped downslope towards the Dead Sea Basin at *c.* 18 ka. We employ five methods of slump transport analysis and note that they all provide consistent results that are typically within 15° of one another at each site. A greater appreciation of the variability that may develop around simple modern basins, such as described here, may permit a better understanding of the complexities observed in ancient and only partially exposed basins where the palaeogeographical setting may be poorly understood, and may also be masked by subsequent tectonics.

This case study represents one of the few regional analyses of slump fold datasets and allows us, for the first time, to recognize a large-scale radial slump system directed towards the depocentre of the Dead Sea as clearly illustrated by bathymetric maps (Fig. 6d). SE-directed slumping is preserved in the north, easterly directed slumping in the central portion, and NE-directed slumping at the southern end of the Dead Sea. In detail, >90% of fold hinges verge broadly towards the east, >95% of fold hinges face upwards towards the east, and >90% of axial planes dip towards the west. These consistent relationships support flow perturbation models in which transport-normal fold hinges are generated by layer-parallel shearing during broadly east-directed slumping. This radial slump pattern highlights not only the reliability and robustness of techniques, but also the variability of slump directions, which vary by more than 90° along the *c.* 100 km western shore of the Dead Sea. The pristine depositional dips of <1° within the Lisan Fm demonstrate that local tectonics has not significantly affected transport directions with time. Thus, although slumps within the Lisan Fm exposed along the entire length of the Dead Sea Basin may be of slightly different (Late Pleistocene) ages, they portray an overall coherent radial pattern because of the absence of local tilting. Assuming that the slumps were triggered by earthquakes that were distributed all over the basin (much like the recent activity), the pattern proves that the shape, and in particular the vergence, of deformed layers is governed by palaeoslope.

We thank J. Levy, together with the Carnegie Trust and the Royal Society of Edinburgh, for travel grants to I.A., and the Israel Science Foundation for grant 1539/08 to S.M. We would like to thank N. Woodcock and T. Debacker for detailed and constructive reviews of this paper, and J. Marshall for careful editing. S.M. would like to acknowledge the Department of Earth Sciences at Durham University for hosting him and facilitating completion of this paper.

References

Agnon, A., Migowski, C. & Marco, S. 2006. Intraclast breccia layers in laminated sequences: recorders of paleo-earthquakes. *In*: Enzel, Y., Agnon, A. & Stein, M. (eds) *New Frontiers in Dead Sea Paleoenvironmental Research*. Geological Society of America, Special Papers, **401**, 195–214.

Almagor, G. & Garfunkel, Z. 1979. Submarine slumping in continental margin of Israel and Northern Sinai. *AAPG Bulletin*, **63**, 324–340.

Alsop, G.I. & Carreras, J. 2007. Structural evolution of sheath folds: a case study from Cap de Creus. *Journal of Structural Geology*, **29**, 1915–1930.

Alsop, G.I. & Holdsworth, R.E. 2002. The geometry and kinematics of flow perturbation folds. *Tectonophysics*, **350**, 99–125.

Alsop, G.I. & Holdsworth, R.E. 2004*a*. Shear zone folds: records of flow perturbation or structural inheritance? *In*: Alsop, G.I., Holdsworth, R.E., McCaffrey, K.J.W. & Hand, M. (eds) *Flow Processes in Faults and Shear Zones*. Geological Society, London, Special Publications, **224**, 177–199.

Alsop, G.I. & Holdsworth, R.E. 2004*b*. The geometry and topology of natural sheath folds: a new tool for structural analysis. *Journal of Structural Geology*, **26**, 1561–1589.

Alsop, G.I. & Holdsworth, R.E. 2006. Sheath folds as discriminators of bulk strain type. *Journal of Structural Geology*, **28**, 1588–1606.

Alsop, G.I. & Holdsworth, R.E. 2007. Flow perturbation folding in shear zones. *In*: Ries, A.C., Butler, R.W.H. & Graham, R.D. (eds) *Deformation of the Continental Crust: the Legacy of Mike Coward*. Geological Society, London, Special Publications, **272**, 77–103.

Alsop, G.I. & Marco, S. 2011. Soft-sediment deformation within seismogenic slumps of the Dead Sea Basin. *Journal of Structural Geology*, **33**, 433–457.

Alsop, G.I., Holdsworth, R.E. & McCaffrey, K.J.W. 2007. Scale invariant sheath folds in salt, sediments and shear zones. *Journal of Structural Geology*, **29**, 1585–1604.

Alsop, G.I., Cheer, D.A., Strachan, R.A., Krabbendam, M., Kinny, P.D., Holdsworth, R.E. & Leslie, A.G. 2010. Progressive fold and fabric evolution associated with regional strain gradients: a case study from across a Scandian ductile thrust nappe, Scottish Caledonides. *In*: Law, R.D., Butler, R.W.H., Holdsworth, R.E., Krabbendam, M. & Strachan, R.A. (eds) *Continental Tectonics and Mountain Building: the Legacy of Peach and Horne*. Geological Society, London, Special Publications, **335**, 253–272.

Bartov, Y., Steinitz, G., Eyal, M. & Eyal, Y. 1980. Sinistral movement along the Gulf of Aqaba—its age and relation to the opening of the Red Sea. *Nature*, **285**, 220–221.

Begin, Z.B., Ehrlich, A. & Nathan, Y. 1974. Lake Lisan, the Pleistocene precursor of the Dead Sea. *Geological Survey of Israel Bulletin*, **63**, 1–30.

Begin, B.Z., Steinberg, D.M., Ichinose, G.A. & Marco, S. 2005. A 40,000 years unchanging of the seismic regime in the Dead Sea rift. *Geology*, **33**, 257–260.

Bradley, D. & Hanson, L. 1998. Paleoslope analysis of slump folds in the Devonian flysch of Maine. *Journal of Geology*, **106**, 305–318.

Bull, S., Cartwright, J. & Huuse, M. 2009. A review of kinematic indicators from mass-transport complexes using 3D seismic data. *Marine and Petroleum Geology*, **26**, 1132–1151.

Canals, M., Lastras, G. *et al.* 2004. Slope failure dynamics and impacts from seafloor and shallow sub-seafloor geophysical data: case studies from the COSTA project. *Marine Geology*, **213**, 9–72.

Collinson, J. 1994. Sedimentary deformational structures. *In*: Maltman, A.J. (ed.) *The Geological Deformation of Sediments*. Chapman & Hall, London, 95–125.

Corbett, K.D. 1973. Open-cast slump sheets and their relationship to sandstone beds in an Upper Cambrian flysch sequence, Tasmania. *Journal of Sedimentary Petrology*, **43**, 147–159.

Coward, M.P. & Potts, G.J. 1983. Complex strain patterns developed at the frontal and lateral tips to shear zones and thrust zones. *Journal of Structural Geology*, **5**, 383–399.

Debacker, T.N., Sintubin, M. & Verniers, J. 2001. Large-scale slumping deduced from structural and sedimentary features in the Lower Palaeozoic Anglo-Brabant fold belt, Belgium. *Journal of the Geological Society, London*, **158**, 341–352.

Debacker, T.N., Dumon, M. & Matthys, A. 2009. Interpreting fold and fault geometries from within the lateral to oblique parts of slumps: a case study from the Anglo-Brabant Deformation Belt (Belgium). *Journal of Structural Geology*, **31**, 1525–1539.

Doig, R. 1991. Effects of strong seismic shaking in lake sediments, and earthquake recurrence interval, Témiscaming, Quebec. *Canadian Journal of Earth Sciences*, **28**, 1349–1352.

Doughty, M., Eyles, N. & Daurio, L. 2010. Earthquake-triggered slumps (1935 Timiskaming M6.2) in Lake Kipawa, Western Quebec Seismic Zone, Canada. *Sedimentary Geology*, **228**, 113–118.

El-Isa, Z.H. & Mustafa, H. 1986. Earthquake deformations in the Lisan deposits and seismotectonic implications. *Geophysical Journal of the Royal Astronomical Society*, **86**, 413–424.

Elliot, C.G. & Williams, P.F. 1988. Sediment slump structures: a review of diagnostic criteria and application to an example from Newfoundland. *Journal of Structural Geology*, **10**, 171–182.

Farrell, S.G. 1984. A dislocation model applied to slump structures, Ainsa Basin, South Central Pyrenees. *Journal of Structural Geology*, **6**, 727–736.

Farrell, S.G. & Eaton, S. 1987. Slump strain in the Tertiary of Cyprus and the Spanish Pyrenees. Definition of palaeoslopes and models of soft sediment deformation. *In*: Jones, M.F. & Preston, R.M.F. (eds) *Deformation of Sediments and Sedimentary Rocks*. Geological Society, London, Special Publications, **29**, 181–196.

Gardner, J.V., Prior, D.B. & Field, M.E. 1999. Humboldt slide—a large shear dominated retrogressive slope failure. *Marine Geology*, **154**, 323–338.

Garfunkel, Z. 1981. Internal structure of the Dead Sea leaky transform (rift) in relation to plate kinematics. *Tectonophysics*, **80**, 81–108.

Gilbert, L., Sanz De Galdeano, C., Alfaro, P., Scott, G. & Lopez Garrido, A.C. 2005. Seismic-induced slump in Early Pleistocene deltaic deposits of the Baza Basin (SE Spain). *Sedimentary Geology*, **179**, 279–294.

Haase-Schramm, A., Goldstein, S.L. & Stein, M. 2004. U–Th dating of Lake Lisan aragonite (late Pleistocene Dead Sea) and implications for glacial East Mediterranean climate change. *Geochimica et Cosmochimica Acta*, **68**, 985–1005.

Hansen, E. 1971. *Strain Facies*. Springer, Berlin.

Heifetz, E., Agnon, A. & Marco, S. 2005. Soft sediment deformation by Kelvin–Helmholtz instability: a case from Dead Sea earthquakes. *Earth and Planetary Science Letters*, **236**, 497–504.

Holdsworth, R.E. 1988. The stereographic analysis of facing. *Journal of Structural Geology*, **10**, 219–223.

Holdsworth, R.E. 1990. Progressive deformation structures associated with ductile thrusts in the Moine Nappe, Sutherland, N Scotland. *Journal of Structural Geology*, **12**, 443–452.

Jackson, C.A.-L. 2011. Three-dimensional seismic analysis of megaclast deformation within a mass transport deposit: implications for debris flow kinematics. *Geology*, **39**, 203–206.

Jones, O.T. 1939. The geology of the Colwyn Bay district: a study of submarine slumping during the Salopian period. *Quarterly Journal of the Geological Society of London*, **380**, 335–382.

Kagan, E., Stein, M., Agnon, A. & Neuman, F. 2011. Intrabasin palaeoearthquake and quiescence correlation of the late Holocene Dead Sea. *Journal of Geophysical Research*, **116**, B04311.

Ken-Tor, R., Agnon, A., Enzel, Y., Marco, S., Negendank, J.F.W. & Stein, M. 2001. High-resolution geological record of historic earthquakes in the Dead Sea basin. *Journal of Geophysical Research*, **106**, 2221–2234.

Lazar, M., Ben-Avraham, Z. & Schattner, U. 2006. Formation of sequential basins along a strike-slip fault—geophysical observations from the Dead Sea basin. *Tectonophysics*, **421**, 53–69.

Lee, H.J., Locat, J. *et al.* 2007. Submarine mass movements on continental margins. *In*: Nittrouer, C.A., Austin, J.A., Field, M.E., Kravitz, J.H., Syvitski, J.P.M. & Wiberg, P.L. (eds) *Continental Margin Sedimentation: from Sediment Transport to Sequence Stratigraphy*. International Association of Sedimentologists, Special Publication, **37**, 213–274.

Lesemann, J.-E., Alsop, G.I. & Piotrowski, J.A. 2010. Incremental subglacial meltwater sediment deposition and deformation associated with repeated ice-bed decoupling: a case study from the Island of Funen, Denmark. *Quaternary Science Reviews*, **29**, 3212–3229.

Lewis, K.B. 1971. Slumping on a continental slope inclined at 1–4°. *Sedimentology*, **16**, 97–110.

Maltman, A. 1984. On the term soft-sediment deformation. *Journal of Structural Geology*, **6**, 589–592.

Maltman, A. 1994*a*. *The Geological Deformation of Sediments*. Chapman & Hall, London.

Maltman, A. 1994*b*. Introduction and overview. *In*: Maltman, A. (ed.) *The Geological Deformation of Sediments*. Chapman & Hall, London, 1–35.

Marco, S. & Agnon, A. 1995. Prehistoric earthquake deformations near Masada, Dead Sea graben. *Geology*, **23**, 695–698.

Marco, S., Stein, M., Agnon, A. & Ron, H. 1996. Long term earthquake clustering: a 50,000 year paleoseismic record in the Dead Sea Graben. *Journal of Geophysical Research*, **101**, 6179–6192.

MARCO, S., HARTAL, M., HAZAN, N., LEV, L. & STEIN, M. 2003. Archaeology, history, and geology of the A.D. 749 earthquake, Dead Sea transform. *Geology*, **31**, 665–668.

MARTINSEN, O.J. 1989. Styles of soft-sediment deformation on a Namurian delta slope, Western Irish Namurian Basin, Ireland. *In*: WHATELEY, M.K.G. & PICKERING, K.T. (eds) *Deltas: Sites and Traps for Fossil Fuels*. Geological Society, London, Special Publications, **41**, 167–177.

MARTINSEN, O.J. 1994. Mass movements. *In*: MALTMAN, A. (ed.) *The Geological Deformation of Sediments*. Chapman & Hall, London, 127–165.

MARTINSEN, O.J. & BAKKEN, B. 1990. Extensional and compressional zones in slumps and slides in the Namurian of County Claire, Eire. *Journal of the Geological Society, London*, **147**, 153–164.

MIGOWSKI, C., AGNON, A., BOOKMAN, R., NEGENDANK, J.F.W. & STEIN, M. 2004. Recurrence pattern of Holocene earthquakes along the Dead Sea transform revealed by varve-counting and radiocarbon dating of lacustrine sediments. *Earth and Planetary Science Letters*, **222**, 301–314.

MOERNAUT, J. & DE BATIST, M. 2011. Frontal emplacement and mobility of subalacustrine landslides: results from morphometric and seismostratigraphic analysis. *Marine Geology*, **285**, 29–45.

POTTER, P.E. & PETTIJOHN, F.J. 1977. *Palaeocurrents and Basin Analysis*. 2nd edn. Academic Press, New York.

RIDLEY, J. 1986. Parallel stretching lineations and fold axes oblique to displacement direction—a model and observations. *Journal of Structural Geology*, **8**, 647–654.

RUPKE, N.A. 1978. Deep clastic seas. *In*: READING, H.G. (ed.) *Sedimentary Environments and Facies*. Blackwell, Oxford, 372–415.

SEILACHER, A. 1984. Sedimentary structures tentatively attributed to seismic events. *Marine Geology*, **55**, 1–12.

SMITH, J.V. 2000. Flow pattern within a Permian submarine slump recorded by oblique folds and deformed fossils, Ulladulla, south-eastern Australia. *Sedimentology*, **47**, 357–366.

STRACHAN, L.J. 2002. Slump-initiated and controlled syndepositional sandstone remobilization: an example from the Namurian of County Clare, Ireland. *Sedimentology*, **49**, 25–41.

STRACHAN, L.J. 2008. Flow transformations in slumps: a case study from the Waitemata Basin, New Zealand. *Sedimentology*, **55**, 1311–1332.

STRACHAN, L.J. & ALSOP, G.I. 2006. Slump folds as estimators of palaeoslope: a case study from the Fisherstreet Slump of County Clare, Ireland. *Basin Research*, **18**, 451–470.

WALDRON, J.W.F. & GAGNON, J.-F. 2011. Recognizing soft-sediment structures in deformed rocks of orogens. *Journal of Structural Geology*, **33**, 271–279.

WETZLER, N., MARCO, S. & HEIFETZ, E. 2010. Quantitative analysis of seismogenic shear-induced turbulence in lake sediments. *Geology*, **38**, 303–306.

WOODCOCK, N.H. 1976*a*. Ludlow Series slumps and turbidites and the form of the Montgomery Trough, Powys, Wales. *Proceedings of the Geologists' Association*, **87**, 169–182.

WOODCOCK, N.H. 1976*b*. Structural style in slump sheets: Ludlow Series, Powys, Wales. *Journal of the Geological Society,* London, **132**, 399–415.

WOODCOCK, N.H. 1979. The use of slump structures as palaeoslope orientation estimators. *Sedimentology*, **26**, 83–99.

Received 8 March 2011; revised typescript accepted 5 July 2011.
Scientific editing by John Marshall.

The Geological Society

serving science & profession

New and Recent Book Titles 2011

For full details see the Online Bookshop: www.geolsoc.org.uk/bookshop

NEW

•ISBN: 978-1-86239-329-5
•July 2011
•pages tbc •Hardback
•Prices:
List: **tbc**
GSL: **tbc**
Other qualifying societies: **tbc**
(Cat no tbc)
Online bookshop code: SP355

• Special Publication 355

The SE Asian Gateway: History and Tectonics of the Australia-Asia collision

Edited by R. Hall, M. Cottam and M. E. J. Wilson

Collision between Australia and SE Asia began in the Early Miocene and reduced the former wide ocean between them to a complex passage which connects the Pacific and Indian Oceans. Today, the Indonesian Throughflow passes through this gateway and plays an important role in global thermohaline flow, and the region around it contains the maximum global diversity for many marine and terrestrial organisms. Reconstruction of this geologically complex region is essential for understanding its role in oceanic and atmospheric circulation, climate impacts, and the origin of its biodiversity.

The papers in this volume discuss the Palaeozoic to Cenozoic geological background to Australia and SE Asia collision, and provide the background for accounts of the modern Indonesian Throughflow, oceanographic changes since the Neogene, and aspects of the region's climate history.

NEW

•ISBN: 978-1-86239-326-4
•May 2011
•264 pages •Hardback
•Prices:
List: **£90.00/US$180.00**
GSL: **£45.00/US$90.00**
Other qualifying societies: **£54.00/US$108.00** *(Cat no tbc)*
Online bookshop code: SP353

• Special Publication 353

Growth and Collapse of the Tibetan Plateau

Edited by R. Gloaguen and L. Ratschbacher

Despite agreement on first-order features and mechanisms, critical aspects of the origin and evolution of the Tibetan Plateau, such as the exact timing and nature of collision, the initiation of plateau uplift, and the evolution of its height and width, are disputed, untested or unknown. This book gathers papers dealing with the growth and collapse of the Tibetan Plateau. The timing, the underlying mechanisms, their interactions and the induced surface shaping, contributing to the Tibetan Plateau evolution are tightly linked via coupled and feedback processes. We therefore present cross-disciplinary contributions which allow insight into the complex interactions between lithospheric dynamics, topography building, erosion, hydrological processes and atmospheric coupling. The book is structured in four parts: early processes in the plateau formation; recent growth of the Tibetan Plateau; mechanisms of plateau growth; and plateau uplift, surface processes and the monsoon.

NEW

•ISBN: 978-1-86239-324-0
•April 2011
•292 pages •Hardback
•Prices:
List: **£100.00/US$200.00**
GSL: **£50.00/US$100.00**
Other qualifying societies: **£60.00/US$120.00** *(Cat no tbc)*
Online bookshop code: SP351

• Special Publication 351

Slope Tectonics

Edited by M. Jaboyedoff

Usually geomorphology, structural geology and engineering geology provide descriptions of slope instability in quite distinctive ways. This new research is based on combined approaches to providing an integrated view of the operative slope processes. 'Slope Tectonics' is the term adopted here to refer to those deformations that are induced or fully controlled by the slope morphology, and that generate features which can be compared to those created by tectonic activity. Such deformation can be induced by the stress field in a slope which is mainly controlled by gravity, topography and the geological setting created by the geodynamic context.

The content of this book includes slope-deformation characterization using morphology and evolution, mechanical behaviour of the material, modes of failure and collapse, influence of lithology and structural features, and the role played by controlling factors. The contributions cover broad aspects of slope tectonics that attempt to underline a multidisciplinary approach, which should create a better framework for studies of slope instability.

NEW

•ISBN: 978-1-86239-320-2
•March 2011
•264 pages •Hardback
•Prices:
List: **£90.00/$180.00**
GSL: **£45.00/$90.00**
Other qualifying societies: **£54.00/$108.00** *(Cat no 1064)*
Online bookshop code: SP349

• Special Publication 349

Kinematic Evolution and Structural Styles of Fold-and-Thrust Belts

Edited by J. Poblet and R. J. Lisle

Fold-and-thrust belts occur worldwide, have formed in all eras of geological time, and are widely recognized as the most common mode in which the crust accommodates shortening. Much current research on the structure of fold-and-thrust belts is focused on structural studies of regions or individual structures and on the geometry and evolution of these regions employing kinematic, mechanical and experimental modelling. In keeping with the main trends of current research, this title is devoted to the kinematic evolution and structural styles of a number of fold-and-thrust belts formed from Palaeozoic to Recent times. The papers included in this book cover a broad range of different topics, from modelling approaches to predict internal deformation of single structures, 3D reconstructions to decipher the structural evolution of groups of structures, palaeomagnetic studies of portions of fold-and-thrust belts, geometrical and kinematical aspects of Coulomb thrust wedges and structural analyses of fold-and-thrust belts to unravel their sequence of deformations.

Order from:
www.geolsoc.org.uk/bookshop

Lyell Collection

The Geological Society's Lyell Collection: journals, Special Publications and books online. For more information visit www.geolsoc.org.uk/LyellCollection